Surface Science 605 (2011) L1–L5

Contents lists available at ScienceDirect

Surface Science

journal homepage: www.elsevier.com/ locate/susc

Surface Science Letters

Spatial point analysis of quantum dot nucleation sites on InAs wetting layer

Tomoya Konishi *, Shiro Tsukamoto

Anan National College of Technology, Anan, Tokushima 774-0017, Japan

ARTICLE INFO

Article history:
Received 6 October 2010
Accepted 31 December 2010
Available online 6 January 2011

Keywords:
Semiconductor
MBE
STM
Wetting layer
Quantum dot
Nucleation
Spatial point analysis
Nearest-neighbor distance

ABSTRACT

We perform spatial point analysis of InAs quantum dot (QD) nucleation sites and surface reconstruction domain patterns on an InAs wetting layer to investigate QD nucleation mechanisms in Stranski-Krastanow growth mode. An InAs wetting layer on a GaAs(001) substrate has been observed at 300 °C by using *in situ* scanning tunneling microscopy (STM) preceding QD formation. A nearest-neighbor analysis of the STM images finds that the point pattern of QD precursors is similar to that of $(1\times3)/(2\times3)$ surface reconstruction domains which are specific to Ga-rich fluctuation. This provides the evidence that InAs QD nucleation is induced by Ga-rich fluctuation within an InAs wetting layer, as a technical implication for site-controlled QD growth for various QD devices.

Semiconductor quantum dots (QDs) have drawn much attention because of applications in low-chirp laser devices [1], solar cells to harvest energy from the entire solar spectrum [2,3], single-photon sources and optical amplifiers in quantum communication [4,5]. Such devices require highly dense and site-controlled QDs to achieve high efficiencies. For example, QD solar cells owe its high conversion efficiency to an intermediate band or a miniband formed by QDs being uniform in size and periodically distributed in all three dimensions [2,3,6]. The most popular and world-wide method to prepare QDs is to use self-assembly of QDs in Stranski-Krastanow (SK) growth mode. It involves, however, random island nucleation on a highly strained wetting layer (WL). It has been difficult to obtain site-controlled QDs in SK mode because little is known of the nucleation mechanisms.

Some atomic-level studies on surface atom dynamics have been carried out to understand the nucleation mechanisms [7–10]. First principle calculations showed that the migration barrier energy of In adatom on GaAs(001) surface is higher than that on 1ML-InAs/GaAs (001) [8,9]. Using kinetic Monte Carlo (kMC) simulations [10], Tsukamoto et al. found that some migrating In adatoms were captured on Ga-rich fluctuation, within an In/Ga mixed layer, to become a nucleation site [11]. To the best of our knowledge, however, there has not been any direct evidence reported that alloy fluctuation becomes a QD nucleation site. It is still vital to investigate WL surface on an atomic scale, in particular the surface reconstruction, preceding QD nucleation.

Since surface reconstruction changes microscopically and dynamically in the course of WL growth [12–14], *in situ* scanning tunneling microscopy (STM) during molecular beam epitaxy (MBE) growth at high temperatures, such as STMBE [15], is one of the powerful tools to observe it. It is reported that fast Fourier transform analysis of atomic-scale *in situ* STM images of InAs WL on a GaAs(001) substrate, as well as reflectance high-energy electron diffraction (RHEED) measurements, has revealed that the surface reconstruction changes from *c* (4×4) to the mixed structure of $(1\times3)/(2\times3)$ domains and (2×4) domains prior to QD formation [11].

Structure models of $(1\times3)/(2\times3)$ and (2×4) surface reconstructions have been investigated by many researchers using core-level photoemission spectroscopy [16], reflectance-difference spectroscopy [17], *ab initio* calculations in a local density approximation [8,17], and STM observations [18,19], which are, however, still under discussion. Fig. 1 shows the schematic diagrams, reproduced from the literature, of some representative surface reconstruction models. The unit cells of (1×3) and (2×3) have one or two of Ga atoms near the surface whereas those of (2×4) have none. In other words, Ga-rich fluctuation in InAs/GaAs WL, which is expected to become QD nucleation sites, likely forms $(1\times3)/(2\times3)$ surface reconstruction domains. It is crucial to investigate the relationship between QD nucleation sites and surface reconstruction domains. It is quite challenging, however, to witness QD formation specific to a certain reconstruction domain using typical STM scanning speeds because QD formation occurs on a dynamically changing reconstruction, over a timescale of a few seconds even at very low WL growth rates. Although statistical method is useful to solve this problem, it has not yet been employed. In this paper, we firstly demonstrate the statistical

* Corresponding author.
E-mail address: konishi@anan-nct.ac.jp (T. Konishi).

0039-6028/$ – see front matter © 2011 Elsevier B.V. All rights reserved.
doi:10.1016/j.susc.2010.12.034

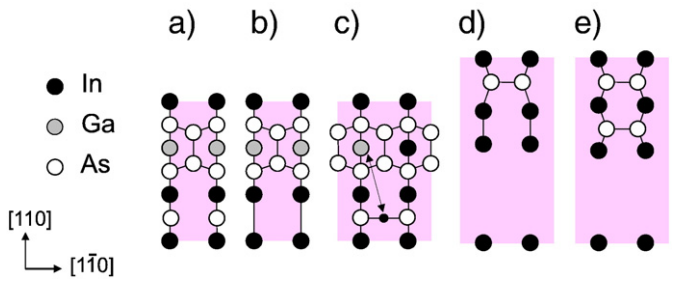

Fig. 1. Schematic diagrams of surface reconstruction models of InAs/GaAs wetting layer on GaAs(001) reproduced from literature: (a) (1×3) [16], (b) (1×3) [17], (c) (2×3) [8], (d) α2(2×4) [18,19], (e) β2(2×4) [18,19]. Background shade indicates unit cell.

comparison of the distribution of surface reconstruction domains and that of QD nucleation sites to investigate the nucleation mechanisms.

The distributions of reconstruction domains and QD nucleation sites are characterized by spatial point patterns; a regular (ordered) pattern, a Poisson (random) pattern, and a clustered (aggregated) pattern [20,21]. In a regular pattern, points are distributed uniformly. A Voronoi tessellation, that is polygonal decomposition of a space by perpendicular bisector lines among neighboring points, is often used in spatial point analysis. The standard deviation of Voronoi cell area, σ_{Vc}, represents point patterns. Examples of spatial point patterns and Voronoi tessellations are illustrated in Fig. 2. Here, we have to be careful of the Voronoi cells touching the boundary of the study region because of the "edge effect," in which contribution from points outside cannot be taken into account. In this study, such invalid Voronoi cells were excluded from the study region. For more precise analysis, second-order properties of point patterns like nearest-neighbor distances are useful [21–24]. Let r denote the distance to the nearest point from a randomly selected location in the study region R. The $F(d)$ function denotes the cumulative frequency distribution of r [21] and hence the probability that r occurs less than any particular distance d. Since the F function is practically identical to the probability of plotting a random point within any of the circles $C_i(d)$, of each radius d, centered on each of the points, it is simply computed by

$$F(d) = \frac{\text{Area}(\cup_i C_i(d) \cap R)}{\text{Area}(R)}, \quad (1)$$

where the numerator is the area of the union of the circles (shaded region in Fig. 2), and the denominator is the area of the study region R. To compare $F(d)$ between different study regions, d should be normalized by the factor f as follows:

$$f = \sqrt{\text{Area}(R)/N}, \quad (2)$$

where N is the number of points [22]. Eqs. (1) and (2) are schematically illustrated in Fig. 2(a).

A piece (11×13×0.6 mm^3) of GaAs(001) crystal was used as a substrate. First the surface was thermally cleaned to remove the oxide

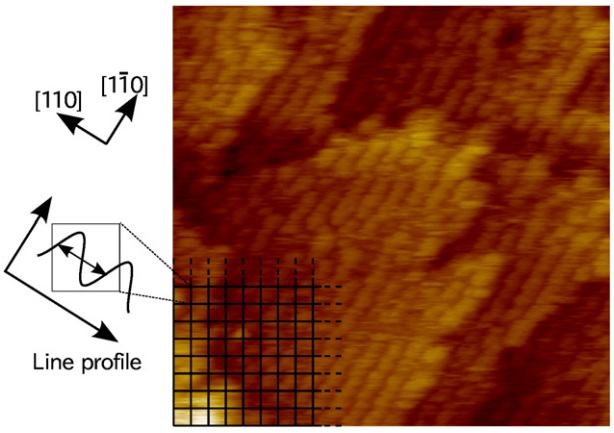

Fig. 3. 30 nm×30 nm filled-state STM image of InAs WL on GaAs(001).

layer under 1×10^{-4} Pa of an As_4 atmosphere in an MBE growth chamber. Next, a GaAs buffer layer was grown on the surface by using MBE until an atomically smooth surface was obtained. The substrate was annealed at 430 °C for 0.5 h to confirm the formation of $c(4\times4)$ reconstruction with RHEED. An STM unit was transferred to the sample holder in the growth chamber and started scanning. This means that the sample was neither cooled to room temperature nor exposed to air to be observed with STM. The tip bias was −3 V and the tunnel current was 0.2 nA. A flux of In was irradiated at the InAs growth rate of 2.5×10^{-4} MLs^{-1}. After a 1.5 monolayer (ML) of InAs WL growth, the substrate temperature was decreased to 300 °C and the As_4 flux was shut off so that the surface reconstruction should be observed in an atomic scale. Another sample was prepared in the same way but SK growth of InAs WL was continued at 430 °C until QD precursors were formed [11]. An STM image of QD precursors was recorded to analyze the distribution of QD nucleation sites.

Fig. 3 shows the filled-state STM image of 1.5 ML of InAs WL recorded at 300 °C. The image seems more or less scratched because of migrating In adatoms on the surface but shows the stripes due to As dimers clearly enough to measure the pitch. The STM image was divided by a 25×25 mesh. The size of each mesh cell was 1.2 nm which is comparable to the unit cell sizes of the InAs WL surface reconstructions as shown in Fig. 4. The stripe pitch was measured from the STM line profile along the [110] azimuth for each mesh cell and plotted in the color map of Fig. 4. The stripe pitch corresponds to the unit cell length along the [110] azimuth of InAs WL surface reconstructions in Fig. 1. The unit cell length of InAs WL is expected to have a similar value to that of the substrate GaAs(001) surface reconstruction, for example, 0.8 nm for $c(4\times4)$, 1.2 nm for (1×3)/(2×3) and 1.6 nm for (2×4). In order to estimate surface reconstruction for each cell, we thus classified the measured pitches using the following three bins: 0.8±0.2 nm assuming $c(4\times4)$, 1.2±0.2 nm assuming (1×3)/(2×3), and 1.6±0.2 nm assuming (2×4), taking account for some deviation by nonuniform surface strain and/or measurement errors. It was found that most cells showed (1×3)/

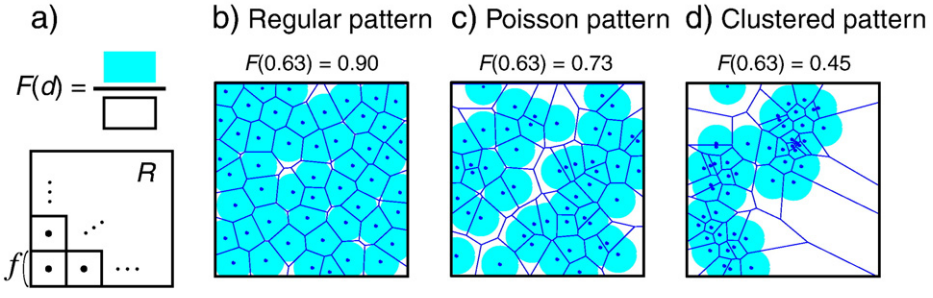

Fig. 2. (a) Schematic illustrations of Eqs. (1) and (2), and examples of $F(d)$ and Voronoi tessellation for (b) regular pattern, (c) Poisson pattern and (d) clustered pattern [22].